Journal of Power Sources 356 (2017) 566–571

Contents lists available at ScienceDirect

Journal of Power Sources

journal homepage: www.elsevier.com/locate/jpowsour

Current density reversibly alters metabolic spatial structure of exoelectrogenic anode biofilms

Dan Sun [a, b, *], Shaoan Cheng [b, **], Fang Zhang [c], Bruce E. Logan [d]

[a] Ocean College, Zhejiang University, Zhoushan 316021, PR China
[b] State Key Laboratory of Clean Energy Utilization, Department of Energy Engineering, Zhejiang University, Hangzhou 310027, PR China
[c] School of Environment, State Key Joint Laboratory of Environment Simulation and Pollution Control, Tsinghua University, Beijing 100084, PR China
[d] Department of Civil and Environmental Engineering, The Pennsylvania State University, University Park, PA 16802, USA

HIGHLIGHTS

- A biofilm with a live outer-layer and dead inner-core was observed under low current.
- A single and completely viable biofilm was observed under high current.
- Switching biofilms between currents produced an outcome associated with the new one.

GRAPHICAL ABSTRACT

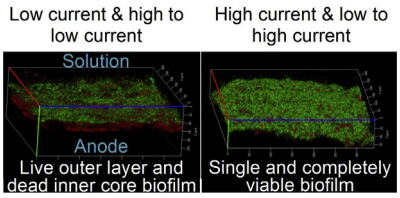

ARTICLE INFO

Article history:
Received 22 October 2016
Received in revised form
29 November 2016
Accepted 30 November 2016
Available online 9 December 2016

Keywords:
Bioelectrochemical system
Anode biofilm
Metabolic structure
Current density
Reversible effect

ABSTRACT

Understanding how current densities affect electrogenic biofilm activity is important for wastewater treatment as current densities can substantially decrease at COD concentrations greater than those suitable for discharge to the environment. We examined the biofilm's response, in terms of viability and enzymatic activity, to different current densities using microbial electrolysis cells with a lower (0.7 V) or higher (0.9 V) added voltage to alter current production. Viability was assessed using florescent dyes, with dead cells identified on the basis of dye penetration due to a compromised cell outer-membrane (red), and live cells (intact membrane) fluorescing green. Biofilms operated with 0.7 V produced 2.4 ± 0.2 A m^{-2}, and had an inactive layer near the electrode and a viable layer at the biofilm-solution interface. The lack of cell activity near the electrode surface was confirmed by using an additional dye that fluoresces only with enzymatic activity. Adding 0.9 V increased the current by 61%, and resulted in a single, more homogeneous and active biofilm layer. Switching biofilms between these two voltages produced outcomes associated with the new current rather than the previous biofilm conditions. These findings suggest that maintaining higher current densities will be needed to ensure long-term viability electrogenic biofilms.

1. Introduction

Bioelectrochemical systems (BESs) are emerging technologies being developed for various applications, including electricity generation in microbial fuel cells (MFCs), biohydrogen production in microbial electrolysis cells (MECs), wastewater treatment, and microbial electrosynthesis of chemicals and biofuels [1–7]. The success of these BES applications relies on anode biofilms that can

* Corresponding author. Ocean College, Zhejiang University, Zhoushan 316021, PR China.
** Corresponding author.
E-mail addresses: dsun@zju.edu.cn (D. Sun), shaoancheng@zju.edu.cn (S. Cheng).

http://dx.doi.org/10.1016/j.jpowsour.2016.11.115
0378-7753/

reliably produce electrical current from organic matter in water [8–12]. The initial growth of exoelectrogenic bacteria on the anode is dependent on the electrode potential, type of substrate, substrate concentration and current density [13–16]. Anode biofilms regularly fed with high concentrations of acetate have been shown to produce stable cycles of current generation even after a year of operation [17]. However, few studies have examined biofilm viability as a function of current generation over time. In applications such as wastewater treatment, the concentration of organic matter is highly variable, and low concentrations of organic matter results in little current production in MFCs [18]. Low current, and thus low growth rates, could impact long-term viability of the biofilm or the ability of exoelectrogenic bacteria to remain predominant in the biofilm compared to the growth of other bacteria sustained by fermentation or respiration with alternate electron acceptors.

Anode communities have been extensively studied in BESs, with most studies showing that high current densities have a predominance of *Geobacter* species which form a conductive biofilm through production of electrically conductive pili [9,10,13,15], or *c*-type cytochrome OmcS [19–22]. The viability of pure and mixed culture biofilms can vary within the biofilm, producing different structures: a live outer-layer with a dead inner-core; a dead outer-layer with a live inner-core; and a completely viable biofilm [16,23,24]. So far, most electroactive biofilm studies have reported either completely viable biofilms or biofilms containing a dead inner layer [24–31]. Current density was identified as a key factor in the development of a dead inner layer, as biofilms grown at a higher current density were completely viable (based on using live/dead stains), whereas lower current densities resulted in a dead inner layer [16]. One limitation of this deduction was that fluorescent dyes used to assess viability were based on membrane integrity, not actual activity or viability [32]. Thus, cell activity was not directly measured. In addition, the ability to re-generate active biofilms was not examined.

Here, the activity and metabolic structure of an electrogenic biofilm was visualized by two different staining methods, for biofilms grown under one voltage (low or high applied voltage) that were switched to the other voltage to study subsequent changes in the viability and activity of the biofilm. The current was varied by using different applied voltages to the circuit, rather than using set potentials or different substrate concentrations, as this approach allowed for simple reactor operation and otherwise relatively similar operating conditions. SYTO9 and propidium iodide (PI) were used to infer viability based on staining color relative to membrane integrity, as done in previous studies [16,26,29,33]. An additional dye, fluorescein diacetate, was used to directly measure cell activity based on the conversion of fluorescein diacetate (FDA), a non-fluorescent esterase, into a fluorescent product (fluorescein) as this only occurs in live cells. Thus, this second method directly identified active cells, rather than membrane integrity. Anodic current, metabolic spatial structure and electrochemical properties were examined in response to the changes in applied voltages in order to discern the changes in metabolic structure coupled to current production.

2. Experimental

2.1. MECs construction and operation

Mini-MECs were constructed as previously described [34]. Anodes were polished 1.5 × 1 × 0.3 cm graphite plates (4.5 cm^2 surface area) [16] while the cathodes (1.5 × 1 cm) were made of stainless steel mesh (Type 304, mesh size 90 × 90).

All reactors were inoculated with domestic wastewater (10% v/v) [16]. The medium used contained (per liter) [35]: 1 g acetate, a 50 mM phosphate buffer solution (PBS, 2.45 g $NaH_2PO_4 \cdot H_2O$, 4.58 g Na_2HPO_4), 0.31 g NH_4Cl, 0.13 g KCl, 12.5 mL Wolfe's minerals [36] and 5 mL Wolfe's vitamin solution [36] (pH 7; conductivity = 7.5 mS cm^{-1}). In order to examine the changes in metabolic structure over time, one set of the reactors was started up with an applied voltage of 0.7 V using a power supply, while the other set operated at a higher voltage of 0.9 V, resulting in an increased current density. After 15 cycles of stable operation, the applied voltages were switched for half of the reactors in both sets (0.7 V → 0.9 V, or 0.9 V → 0.7 V) to alter current production (Table 1). All reactors were operated in fed-batch mode at 30 °C.

MECs were connected in parallel to a power supply, with each individual circuit containing a 10 Ω resistor to determine current. Current was calculated using Ohm's law ($I = U/R$), with current densities based on the total anode area (4.5 cm^2). Ag/AgCl reference electrodes (saturated KCl solution, +197 mV vs a standard hydrogen electrode, SHE) were used to record electrode potentials. All electrode potential values were reported here versus a standard hydrogen electrode (SHE). Twelve reactors were started up at the same time, and individual reactors were sacrificed for biofilm examination. For each set (6 reactors), two reactors were used for SYTO9/PI staining, two were used for FDA/PI staining, and two were used for electrochemical tests. Reactors used for staining tests did not contain a reference electrode in order to minimize possible damage to the biofilm due to the close proximity of the working and reference electrodes. Reactors with electrodes were operated for a total of 15 or 30 cycles.

2.2. Metabolic structure of the anode biofilm

Anodes were stained using a LIVE/DEAD BacLight Bacterial Viability Kit [Invitrogen, CA; SYTO9 and PI fluorescent dyes] to evaluate cell viability based on membrane integrity. Cells stain red when the membrane integrity is compromised, or green when the cells are intact [16,26]. Biofilms were also examined using FDA to assess enzymatic activity, as the cells fluoresce green when FDA is taken up by cells and esterases convert it into fluorescein [37]. These dyes were dissolved in a 50 mM PBS at final concentrations of 10 mg L^{-1} FDA and 30 mg L^{-1} PI. The anodes were operated for 3 min in the dark with these solutions to stain the cells.

After staining, samples were examined with a confocal laser scanning microscope (CLSM) (LSM710 NLO, ZEISS) with a water objective (LD LCI Plan-Apochromat 25 × 0.8 Imm Korr DIC). The whole anode plate was observed by CLSM, and then images were obtained at random locations. The three-dimensional biofilm structure (z-stack) was reconstructed and analyzed using the software ZEN 2009 Light Edition. Anodes were pretreated as previously described [16].

2.3. Electrochemical analysis

Linear sweep voltammetry (LSV), first derivative LSV, and non-turnover cyclic voltammetry (CV) were used to examine the biofilm electrochemical characteristics as previously described [16,38]. Before tests, the liquid in the reactor was removed, and the empty

Table 1
Operation mode of each testing system.

Testing systems	Operation mode
$S_{0.7V}$	15 cycles under 0.7 V
$S_{0.9V}$	15 cycles under 0.9 V
$S_{0.7V \rightarrow 0.9V}$	15 cycles under 0.7 V, and then 15 cycles under 0.9 V
$S_{0.9V \rightarrow 0.7V}$	15 cycles under 0.9 V, and then 15 cycles under 0.7 V

reactor was flushed with N_2, and then refilled with fresh medium for LSV tests, or 50 mM PBS for non-turnover CV tests. For LSV tests, the reactors were set at open circuit conditions for 1 h, and then scanned from −0.50 to +0.30 V at a rate of 1 mV s^{-1}. For CV tests, the reactors were rinsed with 50 mM PBS for 10 min (twice), refilled with 50 mM PBS, set at open circuit conditions for 1 h, and then scanned between −0.50 to +0.30 V at a rate of 1 mV s^{-1}.

3. Results and discussion

3.1. Current generation

Within 15 batch cycles, the MECs operated under a low applied voltage (0.7 V) produced a stable current of 2.4 ± 0.2 A m^{-2}, while the other set of reactors operated at the higher applied voltage (0.9 V) produced a 61% greater current density of 3.8 ± 0.2 A m^{-2} (Fig. 1a). Following this period, the applied voltage on these two sets of reactors were switched and operated for another 15 cycles. After this change, the reactors switched from 0.7 to 0.9 V ($S_{0.7V\rightarrow0.9V}$) increased current to 3.7 ± 0.3 A m^{-2}, while the other set of reactors switched from 0.9 V to the lower voltage of 0.7 V ($S_{0.9V\rightarrow0.7V}$) showed a decrease in current to 2.3 ± 0.3 A m^{-2}. Both these current densities and anode potentials (−0.18 ± 0.01 V at 0.7 V, and −0.12 ± 0.02 V at 0.9 V) were the same as those originally obtained at these two applied voltages (Fig. 1a, and Supplementary Material Fig. S1). This showed that the biofilms could reversibly respond to a new applied voltage, and thus produce the same current density, when operational conditions were changed.

The maximum current densities that could be produced by the anodes was evaluated using LSV (Fig. 1b). Two types of curves resulted from the four different test conditions. All LSVs had typical sigmoidal shapes (Fig. 1b), which is generally thought to be the substrate limited behavior as previously reported in previous CV studies of *Geobacter* and biofilms dominated by *Geobacter* [23,39,40]. The highest current density was obtained from the reactor initially operated at 0.9 V (6.3 ± 0.2 A m^{-2}), which was nearly identical to that of the reactor switched to 0.9 V from 0.7 V. The other two curves that were similar to each other were from the operated at an applied voltage of 0.7 V for the first 15 batches, or after being switched to 0.7 V (originally operated at 0.9 V), with a maximum current density of 5.2 ± 0.1 A m^{-2}. These LSV results further confirmed that the electrochemical activity of anode biofilms was determined primarily in response to acclimation to a specific added voltage, rather than its previous operating conditions.

3.2. Metabolic structure of anode biofilm

To test whether changes in current densities would alter the anode metabolic structure, anode viability and activity was examined using fluorescent stains after 15 cycles at a set voltage. Our results showed that the apparent biofilm viability reversibly varied as a function of applied voltage (Fig. 2, and Fig. S2). At 0.7 V, we observed a two-layer biofilm structure, with a live outer-layer on top at the biofilm-solution interface, and a dead (membrane compromised) inner-core layer near the electrode surface (Fig. 2a). However, at 0.9 V, there was only a single and completely viable biofilm (Fig. 2b). Additional experiments conducted at a lower applied voltage of 0.5 V also showed a two-layer structure, with a thicker inactive layer and a lower current (1.06 ± 0.06 A m^{-2}; Fig. S2). This stratified biofilm structure, showing a live outer-layer and dead inner layer, indicated that the cell growth on the outer layer of thick biofilms was not limited by electrical conductivity, but the cell respiration on the inner layer might be limited by the substrate diffusion to the cells or proton accumulation (low pH)

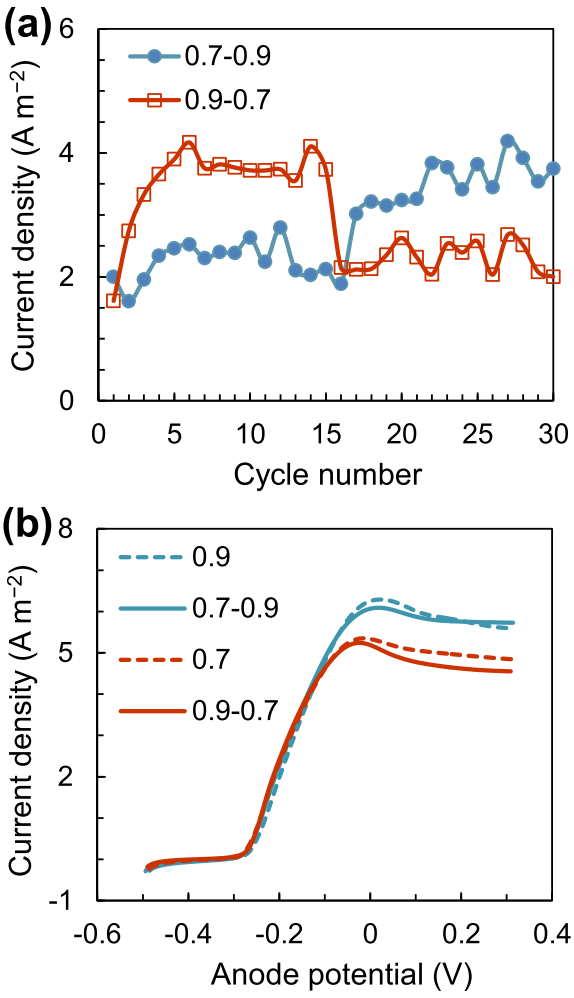

Fig. 1. (a) Current densities recorded for each cycle obtained for mini-MECs operated with the switching applied voltages (0.7 → 0.9 V, or 0.9 → 0.7 V). (b) LSVs (1 mV s^{-1}) of reactors with the applied voltages 0.7 V and 0.9 V, and with the switching applied voltages (0.7 → 0.9 V, or 0.9 → 0.7 V).

[16]. The whole live biofilm structure under 0.9 V indicated that maintaining a high anodic current density would create a high electrochemical pressure condition for biofilm growth, which may be necessary to inhibit accumulation of dead cells.

Anode potentials became more positive at the higher applied voltage (Fig. S1). These changes in potential could also have affected the biofilm growth and current generation. However, higher anode potentials do not necessarily produce more active biofilms, and setting electrode potentials will also impact current densities [13,15]. Although the bacteria can gain more energy from higher anode potentials, the use of higher anode potentials do not necessarily improve current generation or biofilm electrochemical activity. Most research has shown that a higher current will be obtained at a lower anode potential [13,15], while the opposite results were shown in some other studies [41,42]. Moreover, in different studies where the researchers have set the same anode potential (+300 mV vs Ag/AgCl) they found differences in metabolic structure or viability [25,43]. For example, Renslow et al. observed a similar two-layer biofilm structure [43], while Reguera et al. showed a whole live biofilm [25]. Thus, our focus in this work is on the dynamic change (electron generation rate) in the electrochemical and biological response of an active biofilm, rather than just the absolute value of the anode potential. Additional

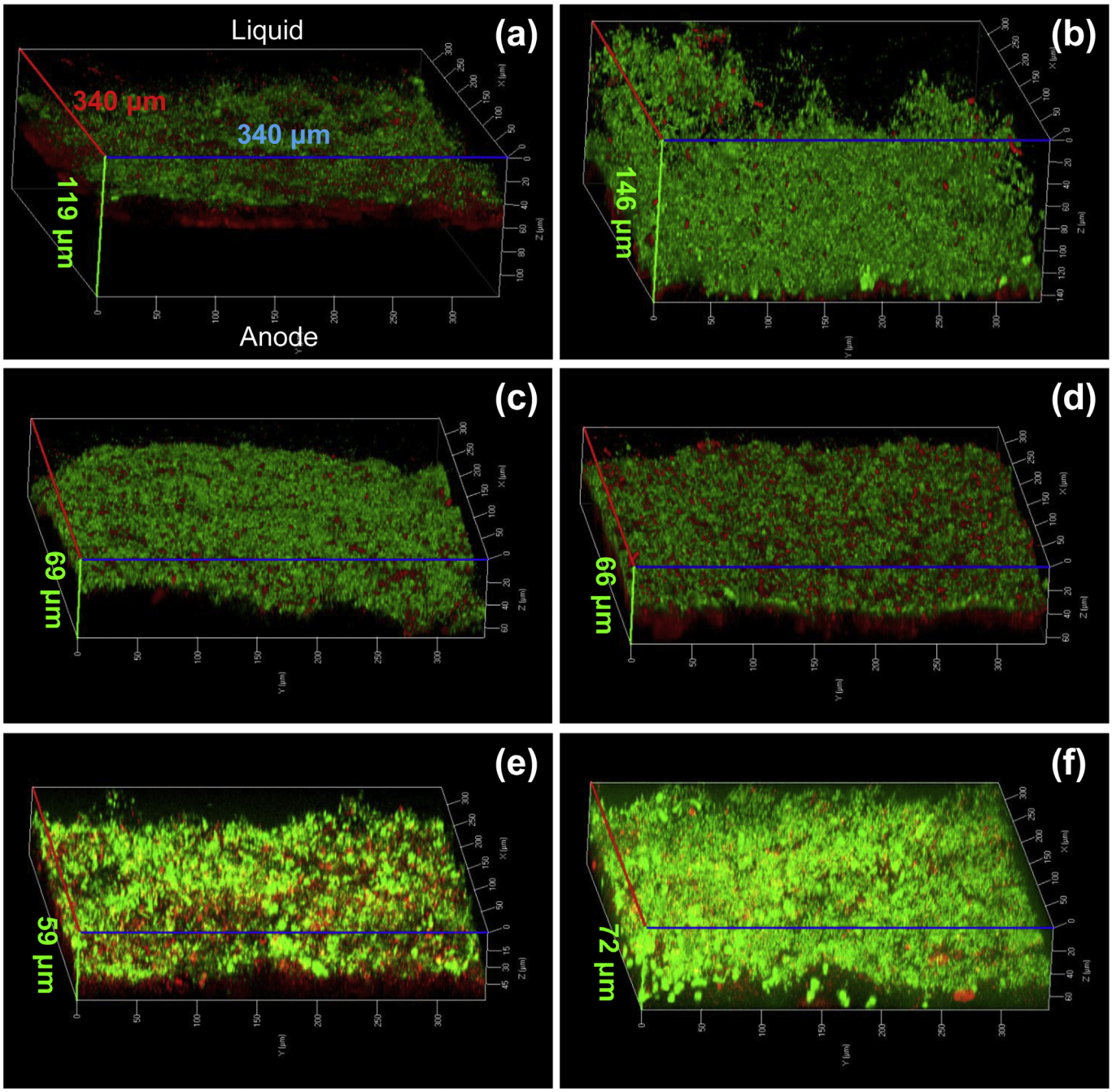

Fig. 2. The 3D metabolic-structure images (bottom surface/inner layer, upper surface/outer layer) of anode biofilms were obtained by using CLSM. The data labeled in the Z axis (green characters) is the scanning range in the thickness direction. Biofilms were viability staining by using a LIVE/DEAD BacLight Bacterial Viability Kit (a–d) or using two fluorescent dyes of FDA and PI (e, f). Live cells were imaged as green, while dead cells were imaged here as red. Biofilm operated with an applied voltage of 0.7 V (a and e), and biofilm operated with an applied voltage of 0.9 V (b and f), and biofilms operated with the switched applied voltages (0.7 → 0.9 V, c; 0.9 → 0.7 V, d). (For interpretation of the references to colour in this figure legend, the reader is referred to the web version of this article.)

studies could help to further elucidate any specific relationship between specific anode potentials on these biofilms. In addition to the metabolic structure of biofilm, the amount of biomass also might be one of factors that impact current generation. However, as we recently showed using the same type of MFC, the thickness of the live biofilm is more important than the biofilm thickness as current reaches a maximum and then declines as the biofilm becomes thicker due to an inactive biofilm layer near the electrode surface [44].

Switching the applied voltages of the two sets of reactors altered the biofilm appearance to match that associated with the previous outcomes based on the magnitude of the applied voltage. Changing the reactors from a low to high applied voltage 15 cycles increased the current ($S_{0.7V\rightarrow0.9V}$) and resulted in the disappearance of the dead biofilm layer for the next 15 cycles, resulting in a completely viable biofilm at the end of the 30 cycles (Fig. 2c). When the voltage was decreased from 0.9 to 0.7 V after 15 cycles, the current decreased, and a two-layer biofilm structure emerged over the next 15 cycles that had a dead (membrane compromised) layer near the electrode surface after a total of 30 cycles, likely as a result of the

accumulation of dead cells in the inner layer of the original biofilm (Fig. 2d). The absence of dead biofilm at the electrode surface could be due to two factors: loss or replacement of the dead biofilm; or re-growth of the cells near the electrode that were originally classified as dead. Of these two possible explanations, the biofilm replacement appears most likely. When the reactors set at a voltage of 0.7 V were changed to a 0.9 V applied voltage, 6–7 batch cycles were needed before current was restored to the same levels observed for other set of reactors that were operated at this 0.9 V (Fig. 1a). Although we did not quantify biofilm losses, we observed biofilm sloughing based on the presence of small red flakes in the solution and on the bottom of the reactor for the $S_{0.7V\rightarrow0.9V}$ test conditions, but not for the other three systems. This suggests loss of the original biofilm and formation of new active biofilm in its place in $S_{0.7V\rightarrow0.9V}$, as the anodes remained covered by biofilm, consistent with previous tests [16]. The non-turnover CV results also supported this hypothesis as discussed below.

To further interrogate the activities of the biofilm in response to the different voltages, cell activity was examined using the FDA dye to probe for enzymatic activity within the biofilm. The results obtained with FDA/PI matched those obtained with the live/dead staining procedure, with two-layer metabolic structure observed with an applied voltage of 0.7 V (Fig. 2e), and a single active biofilm obtained at 0.9 V (Fig. 2f). One disadvantage of the FDA stain, however, was production of fluorescein by suspended bacteria that resulted in a high background fluorescence (Fig. 2e and f and Fig. S3). This relatively high background could have been reduced by decreasing the incubation time (<5 min) [37], but a low exposure time was difficult to achieve due to the time needed to scan the biofilm (5–11 min). The results with the FDA dye, even with this high background in fluorescence, were sufficient to confirm the two-layer structure observed with the live-dead stains.

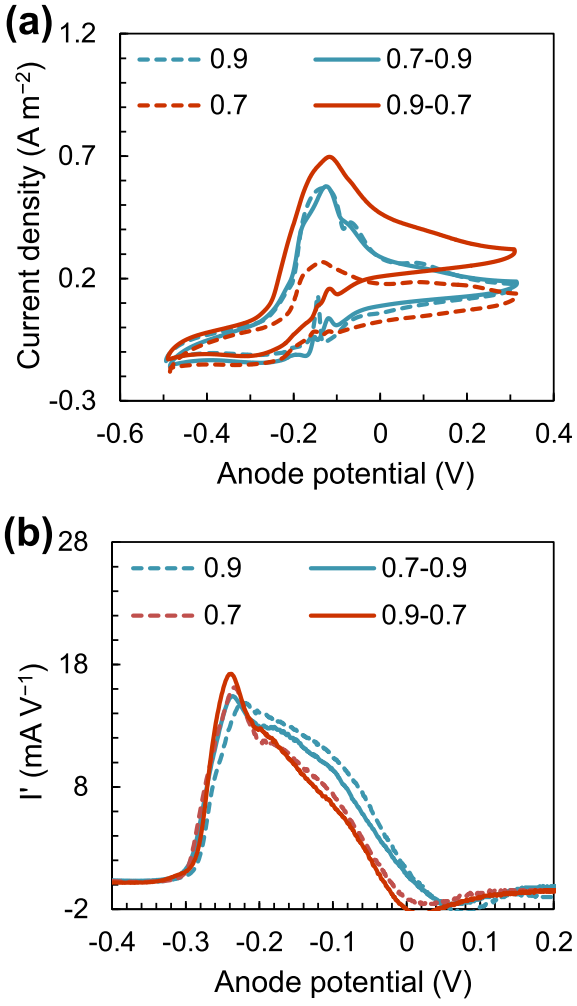

Fig. 3. (a) Non-turnover CV (1 mV s^{-1}) of the reactors with the applied voltages 0.7 V and 0.9 V, and with the switching applied voltages (0.7 → 0.9 V, or 0.9 → 0.7 V). (b) First derivative analysis of LSV curves from Fig. 1b.

3.3. Electrochemical properties of anode biofilm

Non-turnover CV tests with no acetate in 50 mM PBS (unlike LSV tests where acetate was present) were performed to evaluate the presence of redox active components (mediators) within the biofilms. Our previous study showed that under the same condition, the peak current densities measured in non-turnover CVs increased with the total biomass rather than live biomass in the biofilm [16], since dead cells still have redox active components to transfer electrons, but not generate electrons. For reactors operated only an applied voltage of 0.9 V for the first 15 cycles, or those switched from 0.7 to 0.9 V for cycles 16 through 30, the CVs were nearly identical. This suggests that there was no net increase in biomass (due to sloughing off of old biomass and growth of new biomass in the last 15 cycles, so that the effective growth time was only the last 15 cycles) for reactors switched to 0.9 V ($S_{0.7V\rightarrow0.9V}$) compared to that obtained after 15 batch cycles for biofilms that were always at 0.9 V ($S_{0.9V}$), consistent with the biofilm replacement observed as discussed above. However, the CVs for the reactors only operated at 0.7 V were different from those switched from 0.9 to 0.7 V. The reactors switched to 0.7 V showed a much higher peak current that those always operated at 0.7 V, suggesting more abundant redox active species or biomass in that biofilm (Fig. 3a). This is because the reversible transformation from the whole live structure (0.9 V) to a bi-layer metabolic structure (0.7 V) resulted in dead cells in the inner layer of the original biofilm. Thus the redox active components within the biofilm in $S_{0.9V\rightarrow0.7V}$ continuously built up during the following 15 cycles at 0.7 V (The growth time of $S_{0.9V\rightarrow0.7V}$ are 15 cycles at 0.9 V and then 15 cycles at 0.7 V), leading to a higher CV peak current than those that were started up at 0.7 V for 15 cycles.

The peak current densities were different in non-turnover CVs tests and in LSVs tests, but the similar curve shapes were obtained from four different biofilms in both tests (Fig. 3). One main oxidization peak of *ca.* −0.12 V was observed in non-turnover CVs (Fig. 3a), while similar midpoint potentials of about −0.24 to −0.22 V (Fig. 3b) were achieved in the first derivative LSVs. This indicated that the same redox proteins might be involved in the extracellular electron transfer for four different conditions.

4. Conclusions

Our results demonstrated that the metabolic activity of anode biofilms will change in response to the current. When the current was increased from 2.3 to 3.8 A m^{-2} by changing the applied voltage from 0.7 to 0.9 V, the two-layer structure changed to a uniformly viable and active biofilm. Conversely, when the current was decreased, the biofilm developed an inactive (non-viable) layer of biofilms on the electrode surface. If MECs or MFCs are used for wastewater treatment, the current densities can sharply decrease at lower COD concentrations. The implications of exposure to these lower CODs and current densities could result in development of non-viable cells near the electrode. However, it was also seen that the biofilms activity can be restored at higher current densities. The time scales over which biofilm viability might change, and ways to quickly restore biofilm viability, should be examined to improve reactor performance.

Acknowledgements

We thank Shelong Zhang for assistance with the CLSM imaging. This research was supported by the National Natural Science Foundation of China (Grant Nos. 51408541 and 51278448) and the Zhejiang Provincial Natural Science Foundation of China (Grant No. LY17D060004).

Appendix A. Supplementary data

Supplementary data related to this article can be found at http://dx.doi.org/10.1016/j.jpowsour.2016.11.115.

References

[1] B.E. Logan, K. Rabaey, Science 337 (2012) 686–690.
[2] B.E. Logan, M.J. Wallack, K.-Y. Kim, W. He, Y. Feng, P.E. Saikaly, Environ. Sci. Technol. Lett. 2 (2015) 206–214.
[3] H. Liu, S. Grot, B.E. Logan, Environ. Sci. Technol. 39 (2005) 4317–4320.
[4] R. Cusick, B. Bryan, D. Parker, M. Merrill, M. Mehanna, P. Kiely, G. Liu, B. Logan, Appl. Microbiol. Biotechnol. 89 (2011) 2053–2063.
[5] K.P. Nevin, T.L. Woodard, A.E. Franks, A.M. Summers, D.R. Lovley, mBio 1 (2010) 1–4.
[6] W. Yang, W. He, F. Zhang, M.A. Hickner, B.E. Logan, Environ. Sci. Technol. Lett. 1 (2014) 416–420.
[7] Z. Ge, J. Li, L. Xiao, Y. Tong, Z. He, Environ. Sci. Technol. Lett. 1 (2014) 137–141.
[8] Z.-C. Yang, Y.-Y. Cheng, F. Zhang, B.-B. Li, Y. Mu, W.-W. Li, H.-Q. Yu, Environ. Sci. Technol. Lett. 3 (2016) 133–137.
[9] M.D. Yates, P.D. Kiely, D.F. Call, H. Rismani-Yazdi, K. Bibby, J. Peccia, J.M. Regan, B.E. Logan, ISME J. 6 (2012) 2002–2013.
[10] D.R. Lovley, Annu. Rev. Microbiol. 66 (2012) 391–409.
[11] E. Marsili, J. Sun, D.R. Bond, Electroanalysis 22 (2010) 865–874.
[12] Z. Ren, R.P. Ramasamy, S.R. Cloud-Owen, H. Yan, M.M. Mench, J.M. Regan, Bioresour. Technol. 102 (2011) 416–421.
[13] C.I. Torres, R. Krajmalnik-Brown, P. Parameswaran, A.K. Marcus, G. Wanger, Y.A. Gorby, B.E. Rittmann, Environ. Sci. Technol. 43 (2009) 9519–9524.
[14] P.D. Kiely, J.M. Regan, B.E. Logan, Curr. Opin. Biotech. 22 (2011) 378–385.
[15] D. Sun, D.F. Call, P.D. Kiely, A. Wang, B.E. Logan, Biotechnol. Bioeng. 109 (2012) 405–414.
[16] D. Sun, S. Cheng, A. Wang, F. Li, B.E. Logan, K. Cen, Environ. Sci. Technol. 49 (2015) 5227–5235.
[17] F. Zhang, D. Pant, B.E. Logan, Biosens. Bioelectron. 30 (2011) 49–55.
[18] X. Zhang, W. He, L. Ren, J. Stager, P.J. Evans, B.E. Logan, Bioresour. Technol. 176 (2015) 23–31.
[19] J.P. Busalmen, A. Esteve-Núñez, A. Berná, J.M. Feliu, Angew. Chem. Int. Ed. 47 (2008) 4874–4877.
[20] Y. Liu, D.R. Bond, ChemSusChem 5 (2012) 1047–1053.
[21] D. Millo, F. Harnisch, S.A. Patil, H.K. Ly, U. Schröder, P. Hildebrandt, Angew. Chem. Int. Ed. 50 (2011) 2625–2627.
[22] B. Virdis, D. Millo, B.C. Donose, D.J. Batstone, PLoS One 9 (2014) e89918.
[23] E. Marsili, J.B. Rollefson, D.B. Baron, R.M. Hozalski, D.R. Bond, Appl. Environ. Microbiol. 74 (2008) 7329–7337.
[24] A.E. Franks, K.P. Nevin, R.H. Glaven, D.R. Lovley, ISME J. 4 (2010) 509–519.
[25] G. Reguera, K.P. Nevin, J.S. Nicoll, S.F. Covalla, T.L. Woodard, D.R. Lovley, Appl. Environ. Microbiol. 72 (2006) 7345–7348.
[26] N.S. Malvankar, M. Vargas, K.P. Nevin, A.E. Franks, C. Leang, B.C. Kim, K. Inoue, T. Mester, S.F. Covalla, J.P. Johnson, V.M. Rotello, M.T. Tuominen, D.R. Lovley, Nat. Nanotechnol. 6 (2011) 573–579.
[27] A.E. Franks, K.P. Nevin, H. Jia, M. Izallalen, T.L. Woodard, D.R. Lovley, Energy Environ. Sci. 2 (2009) 113–119.
[28] A.E. Franks, R.H. Glaven, D.R. Lovley, ChemSusChem 5 (2012) 1092–1098.
[29] Y. Liu, H. Kim, R. Franklin, D.R. Bond, Energy Environ. Sci. 3 (2010) 1782–1788.
[30] Y. Liu, H. Kim, R.R. Franklin, D.R. Bond, ChemPhysChem 12 (2011) 2235–2241.
[31] N.S. Malvankar, J. Lau, K.P. Nevin, A.E. Franks, M.T. Tuominen, D.R. Lovley, Appl. Environ. Microbiol. 78 (2012) 5967–5971.
[32] P.N. Tawakoli, A. Al-Ahmad, W. Hoth-Hannig, M. Hannig, C. Hannig, Clin. Oral. Invest 17 (2012) 841–850.
[33] K.P. Nevin, H. Richter, S.F. Covalla, J.P. Johnson, T.L. Woodard, A.L. Orloff, H. Jia, M. Zhang, D.R. Lovley, Environ. Microbiol. 10 (2008) 2505–2514.
[34] D.F. Call, B.E. Logan, Biosens. Bioelectron. 26 (2011) 4526–4531.
[35] D. Sun, D. Call, A. Wang, S. Cheng, B.E. Logan, Environ. Microbiol. Rep. 6 (2014) 723–729.
[36] S. Cheng, D. Xing, D.F. Call, B.E. Logan, Environ. Sci. Technol. 43 (2009) 3953–3958.
[37] X. Xiao, Z. Han, Y. Chen, X. Liang, H. Li, Y. Qian, Phys. Chem. Earth 36 (2011) 424–429.
[38] A.J. Bard, L.R. Faulkner, Electrochemical Methods: Fundamentals and Applications, second ed., John Wiley & Sons, New York, 2001.
[39] K. Fricke, F. Harnisch, U. Schroder, Energy Environ. Sci. 1 (2008) 144–147.
[40] H. Richter, K.P. Nevin, H. Jia, D.A. Lowy, D.R. Lovley, L.M. Tender, Energy Environ. Sci. 2 (2009) 506–516.
[41] D.A. Finkelstein, L.M. Tender, J.G. Zeikus, Environ. Sci. Technol. 40 (2006) 6990–6995.
[42] J.P. Busalmen, A. Esteve-Nunez, J.M. Feliu, Environ. Sci. Technol. 42 (2008) 2445–2450.
[43] R.S. Renslow, J.T. Babauta, A.C. Dohnalkova, M.I. Boyanov, K.M. Kemner, P.D. Majors, J.K. Fredrickson, H. Beyenal, Energy Environ. Sci. 6 (2013) 1827–1836.
[44] D. Sun, J. Chen, H. Huang, W. Liu, Y. Ye, S. Cheng, Int. J. Hydrogen Energy 41 (2016) 16523–16528.